Mixing in the D^0 System Results from Collider Experiments

Monika Grothe*
European Organization for Nuclear Research CERN, EP division
1211 Geneva 23, Switzerland

Abstract

Mixing in the D^0 system may provide a sensitive probe for new physics beyond the Standard Model (SM) but has so far eluded experimental observation. The SM predictions are typically small ($< 10^{-3}$) for the mixing parameters x, y which, in the absence of charge-parity (CP) symmetry violation, measure the mass ($x = \Delta m/\Gamma$) and lifetime ($y = \Delta\Gamma/2\Gamma$) difference of the CP eigenstates in the D^0 system. The asymmetric B-factory experiments BABAR and Belle open up the opportunity of measuring x, y with unprecedented statistical precision and sample purities. Results from BABAR and Belle, and from CLEO are reviewed.

*E-mail: Monika.Grothe@cern.ch

Contents

1 Introduction

Mixing phenomena, i.e. the oscillation of a neutral meson into its corresponding anti-meson as a function of time, have been observed in the K^0 and B^0 systems [1]. Up to now, oscillations in the D^0 system have eluded experimental detection.

This is in keeping with the Standard Model (SM) prediction that mixing in the D^0 system should be substantially smaller than for the K^0 and B^0 [2, 3]. The SM prediction, as discussed below, is a consequence of D^0 - $\overline{D^0}$ mixing being dominated by intermediate states with light d and s quarks, a feature unique to the D^0 system among the neutral mesons.

Mixing phenomena are characterized by two dimensionless parameters x, y. When charge-parity (CP) symmetry holds, they correspond to the difference in mass ($x = \Delta m/\Gamma$) and lifetime ($y = \Delta\Gamma/2\Gamma$) of the CP eigenstates in the neutral meson system. Calculations within the SM typically predict that $|x|, |y| < 10^{-3}$ for the D^0 [4]. Due to the smallness of the SM prediction, mixing in the D^0 system may provide a sensitive probe for physics beyond the SM.

Independent of their discovery potential, precise measurements of x and y in the D^0 system are desirable because even SM predictions for x, y span several orders of magnitude [4]. The main challenge in SM calculations of D^0 - $\overline{D^0}$ mixing is estimating the size of SU(3) flavor-symmetry breaking effects (see below) [3].

In this article, measurements of the mixing parameters x, y in the D^0 system are reviewed. Results on CP violation are only discussed when they arise as integral part of the x, y measurements.

The most recent results come from the asymmetric B-factory experiments BABAR and Belle, in operation since 1999. BABAR, at the storage ring PEP-II of the Stanford Linear Accelerator Center (SLAC), USA, and Belle, at the KEK B-factory in Tsukuba, Japan, have accumulated the largest currently available charm samples (integrated luminosity ~ 100 fb^{-1} by the end of 2002) and can be expected to continue data taking till the end of the decade. Hence, BABAR and Belle open up the opportunity of studying charm decays with unprecedented statistical precision.

The first collider experiment to employ the methods for measuring x, y now in use at BABAR and Belle was the CLEO experiment at the Cornell Electron Storage Ring (CESR), USA, in operation until 1999. This review describes these methods and the results obtained by CLEO, BABAR and Belle. Wherever appropriate, comparisons are made with results from fixed-target experiments, notably from E791 and FOCUS, that were dedicated to

charm studies during the 1991/1992 (E791) and 1996/1997 (FOCUS) fixed-target runs at Fermilab.

2 Mixing formalism

Mesons are produced in strong and electromagnetic interactions as flavor eigenstates with a well-defined quark content. The production Hamiltonian is of the form $\mathcal{H}_0 = \mathcal{H}_{strong} + \mathcal{H}_{em}$. Its eigenstates are the flavor or interaction eigenstates M^0, $\overline{M^0}$. The CPT theorem requires that particle and anti-particle have the same mass and lifetime. Thus M^0 and $\overline{M^0}$ correspond to identical eigenvalues m_0, γ_0 of $\mathcal{H}_0$.

Mesons are observed by way of their decays which are governed by the weak force. The eigenstates of the evolution Hamiltonian that is responsible for their decay, $\mathcal{H} = \mathcal{H}_0 + \mathcal{H}_{weak}$, are the mass or decay eigenstates $M_{1,2}$ with the corresponding eigenvalues $m_{1,2}$ and $\gamma_{1,2}$. They are the physically observable states that obey an exponential decay law with a slope given by the respective lifetime $\gamma_{1,2}$:

$$|M_{1,2}(t)\rangle = |M_{1,2}(0)\rangle e^{-im_{1,2}t} e^{-(\gamma_{1,2}/2)t}. \tag{1}$$

As a consequence of the difference between production and evolution Hamiltonian, a sample of neutral mesons, produced, e.g., as a pure M^0 sample, evolves in time as a superposition of M^0 and $\overline{M^0}$ states with time-dependent coefficients:

$$|M(t)\rangle = c_{M^0}(t)|M^0\rangle + c_{\overline{M^0}}(t)|\overline{M^0}\rangle. \tag{2}$$

The time evolution obeys Schrödinger's equation:

$$\frac{\partial}{\partial t}\begin{pmatrix} c_{M^0}(t) \\ c_{\overline{M^0}}(t) \end{pmatrix} = -i\mathcal{H}\begin{pmatrix} c_{M^0}(t) \\ c_{\overline{M^0}}(t) \end{pmatrix} \quad \text{with } \mathcal{H} = \begin{bmatrix} m_0 - i\frac{\gamma_0}{2} & m_{12} - i\frac{\Gamma_{12}}{2} \\ m_{12}^\star - i\frac{\Gamma_{12}^\star}{2} & m_0 - i\frac{\gamma_0}{2} \end{bmatrix}. \tag{3}$$

This equation represents two coupled differential equations. Its eigenstates are the physically observable eigenstates $M_{1,2}$. As a consequence of the non-zero off-diagonal elements in the Hamiltonian $\mathcal{H}$, the mass eigenstates $M_{1,2}$ are obtained as linear superpositions of the flavor eigenstates:

$$|M_{1,2}\rangle = p|M^0\rangle \pm q|\overline{M^0}\rangle. \tag{4}$$

In the absence of CP violation, i.e. for $q/p = 1$, $M_{1,2}$ are CP eigenstates.

For a more detailed discussion, see Ref. [5].

2.1 The mixing parameters x, y

Mixing phenomena can be characterized by two dimensionless parameters:

$$y = (\gamma_1 - \gamma_2)/(\gamma_1 + \gamma_2) = \Delta\Gamma/2\Gamma, \qquad x = (m_1 - m_2)/\Gamma = \Delta m/\Gamma. \quad (5)$$

Mixing in a neutral meson system occurs when at least one of the two following possibilities applies: Between the decay eigenstates of the system there is a non-zero lifetime difference ($y \neq 0$), or there is a non-zero mass difference ($x \neq 0$). In the first case, flavor mixing is a consequence of the shorter-living decay eigenstate dying out. The remaining longer-living one is a linear combination of a M^0 and a $\overline{M^0}$ component, so that even an initially pure M^0 sample shows some fraction of $\overline{M^0}$ after some time. In the second case, flavor mixing is a consequence of a pure transition from M^0 to $\overline{M^0}$ and vice versa.

In the D^0 system, according to the SM, CP violation is a negligible effect (see below); the decay eigenstates are, to a good approximation, also CP eigenstates. In the following, the eigenstate D_1 (D_2) with mass m_1 (m_2) and width γ_1 (γ_2) is chosen as CP-even (CP-odd).[a] In the K^0 and B^0 systems, where CP violation is experimentally observable [6], the conventional choice for K_1 and B_1 (K_2 and B_2) is the heavier (lighter) eigenstate.

In oscillation plots that show the fraction of $\overline{M^0}$ flavor states in an initially pure sample of M^0 as a function of time, the parameter x is related to the frequency of the oscillation, while y is related to the damping of its amplitude.

The two parameters x, y reflect different mechanisms through which mixing can proceed in lowest order in the SM [7]. A M^0 can oscillate into its anti-particle by way of on-shell intermediate states that are accessible to both particle and anti-particle. These are long-range processes with amplitudes $\propto -iy$. On the other hand, a M^0 can also oscillate by way of off-shell intermediate states that can be represented by box-diagram loops (see Fig. 1). These are short-range processes with amplitudes $\propto x$. Additional contributions to the box diagrams in Fig. 1(right) from as-of-yet unobserved non-SM particles could result in a deviation of the measured value of x from the SM prediction.

The time-integrated probability of a neutral meson to oscillate first and then decay compared to decaying directly is described by the mixing rate R_{mix}. In the absence of CP violation in mixing, R_{mix} is identical for M^0 and $\overline{M^0}$. The following expression then holds for the decay of a M^0 into a

[a] This convention follows the one used by the CLEO collaboration [7].

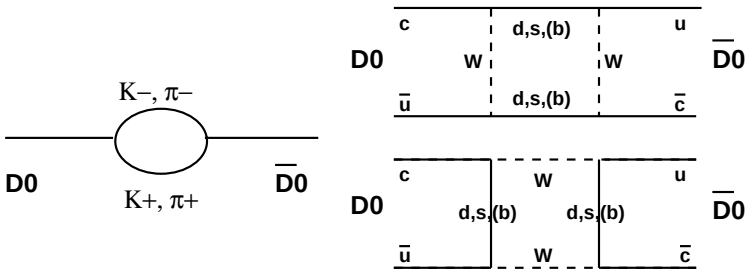

Figure 1: The types of processes through which mixing can proceed in lowest order in the SM. Left: Long range processes with amplitude $\propto -iy$. Right: Short range processes with amplitude $\propto x$ [7].

final state f [5]:

$$R_{mix} = \mathcal{B}(M^0 \to \overline{M^0} \to \bar{f}) \;/\; \mathcal{B}(M^0 \to f) = (x^2 + y^2)/(2 + x^2 - y^2). \quad (6)$$

In the D^0 system, the SM expectations for $|x|$ and $|y|$ are typically below 10^{-3}, which results in $R_{mix}(D^0) < 10^{-6}$. This explains why up to now no direct observation of flavor mixing in the D^0 system has been achieved and why such an observation is likely to be unaccessible also in the future if no non-SM effects come into play.

The situation is much more favorable in the K^0 and B^0 systems. Experimentally [1], x and $-y$ are known to be of the order unity for the K^0 system, which implies $R_{mix}(K^0) \sim 1$. In the B^0 system, $x \sim 0.7$ experimentally [1], while $y/x \sim -1/500$ is expected [5], resulting in $R_{mix}(B^0) \sim 0.2$.[b]

2.2 Predictions for mixing in the D^0 system

Predictions for x and y both within and beyond the SM span several orders of magnitude. For a compilation of predicted values, see Ref. [4]. SM predictions give typically $|x|, |y| < 10^{-3}$ and can be as low as 10^{-8}. Contributions of physics beyond the SM may enhance $|x|$ to values of up to 10^{-2}, while $|y|$ is assumed to be dominated by SM effects.

At the source of the large uncertainties in the theoretical description, even within the SM, is the charm mass being intermediate between heavy and light. The charm quark is too light for perturbative treatments to work

[b] For the B_s^0 system, only upper limits have been determined experimentally [1]: $x > 19.0$ at 95% CL, while again $y/x \sim -1/500$ is expected [5], so that $R_{mix}(B_s^0) \sim 1$. Direct experimental observation of mixing in the B_s^0 system is complicated by the very high oscillation frequency $\propto x$.

well but, on the other hand, it is too heavy for its decays to be dominated by a small number of final states. For a detailed discussion, see Ref. [2, 3].

In the SM, the D^0 has the unique feature that its mixing proceeds via intermediate states of down-type quarks in the box diagrams of Fig. 1. The contribution of the bottom quark to the loops can be neglected because of the smallness of [8] $V_{ub} \times [(m_b^2 - m_d^2)^2/m_W^2 m_c^2]$. The first factor, V_{ub}, is the coupling between quarks of the first and third generation as described by the Cabibbo-Kobayashi-Maskawa (CKM) matrix. The second factor corresponds to GIM-type suppressions in the loop (see below). Consequently, the D^0 system can be treated to a good approximation as a mere two-generation problem that the SM describes with the help of a 2×2 rotation matrix. There, the rotation angle is the Cabibbo angle θ_C, and no CP violating parameters are foreseen.

In that framework, the D^0 decay is Cabibbo-favored, while the box diagrams of Fig. 1(right) are doubly Cabibbo-suppressed. Thus in the D^0 system, the SM disfavors mixing as expressed by x at least to the level $\sin\theta_C{}^2 \approx 0.05$. In the SU(3) flavor limit, where for the quark masses holds: $m_u = m_d = m_s$, the sum over the box diagrams in Fig. 1(right) is zero (GIM-type cancellation[c]) and x would be zero accordingly. In the SM, where $SU(3)$ flavor symmetry is broken, GIM-type cancellations result in suppression factors that depend on the mass of the heaviest quark in the loop relative to the W boson mass: $(m_s^2 - m_d^2)^2/m_W^2 m_c^2 \sim m_s^2/m_W^2$ for the D^0, as compared to $\sim m_t^2/m_W^2$ ($\sim m_c^2/m_W^2$) for the B^0 (K^0).

For the on-shell intermediate states of Fig. 1(left), which correspond to mixing in the D^0 system as expressed by y, light quark states are favored by phase space. While the limited available phase space for decays results in a large lifetime difference in the K^0 system ($y \sim 1$), such constraints for decays in the D^0 or B^0 system are much weaker. The measured branching ratios for D^0 decays, e.g. into $\pi^+\pi^-$, K^+K^- or $K_s^0\pi^0$ are small and not comparable to the ones in the K^0 system. Based on the same GIM-type suppression arguments as for x, SM predictions typically arrive at $|y| < 10^{-3}$. However, as for $|x|$, the precise size of these GIM-type suppressions is a major source of uncertainty. Recent theoretical work [2, 3] points out the possibility that SU(3) flavor breaking may result in $|y| \sim 0.01$ being natural in the SM. Such a large value of $|y|$ would lower the sensitivity of experimental measurements of D^0 mixing to potential non-SM physics effects in $|x|$.

[c]GIM cancellation led Glashow, Illiopoulos and Maiani to infer from the measured small size of the ratio $BR(K_L^0 \to \mu^+\mu^-)/BR(K_L^0 \to \text{all modes})$ the existence of a fourth quark, the charm quark.

3 Methods for determining x, y in the D^0 system

Given the smallness of the expected mixing rate, R_{mix}, in the D^0 system, the extraction of the mixing parameters from a direct observation of flavor oscillations as a function of time is not feasible. Instead, three complementary methods have been applied by experiments:[d]

1. By comparing the lifetimes measured in hadronic D^0 decays of specific CP symmetry, y can be determined.

2. Measurements using the wrong-sign D^0 decays:
   (a) From the time evolution of wrong-sign hadronic decays, e.g. $D^0 \to K^+\pi^-$, x'^2 and y' can be determined independently. x', y' are related to x, y by a rotation.
   (b) From wrong-sign semileptonic decays, e.g. $D^0 \to K^+ l^- \bar{\nu}_l$, the linear combination $x^2 + y^2$ can be determined.

In order to compare directly the results of method 2(a) to those of methods 1, 2(b), an assumption is necessary for the size of the rotation angle (see below) between x, y and x', y'.

The results of BABAR, Belle and CLEO were obtained with the first two methods. They are discussed in detail in the following. Comparisons to earlier results by FOCUS (methods 1, 2(a)) and E791 (all three methods) are given where appropriate.

BABAR, Belle and CLEO use for their measurements the following hadronic two-prong decays of the D^0:

- The Cabibbo-favored (CF), so-called right-sign (RS) decay $D^0 \to K^-\pi^+$.

- The CP-even decays $D^0 \to K^-K^+$ and $D^0 \to \pi^-\pi^+$ which are singly Cabibbo-suppressed. The former (latter) occurs $\sim 1/9$ ($\sim 1/25$) times less frequently than the RS decay.[e]

- The so-called wrong-sign (WS) decay $D^0 \to K^+\pi^-$ which, in the absence of mixing, is doubly Cabibbo-suppressed (DCS) and occurs $\sim 1/300$ times less frequently than the RS decay.

[d] The charge conjugate modes are always implied unless stated otherwise. The experiments treat D^0 and $\overline{D^0}$ separately only when investigating the possibility of CP violating effects.

[e] In the limit of SU(3) flavor symmetry, the branching ratios for the D^0 decays into K^-K^+ and $\pi^-\pi^+$ are identical. The experimentally observed substantial difference is an example of large SU(3) flavor breaking effects in the D^0 system [9].

3.1 Measurement of y from a D^0 lifetime ratio

In the absence of CP violation, the final state of the RS D^0 decay is an equal mixture of CP-even and CP-odd states. Under the assumption that x and y are small, the decay-time distribution is approximately exponential [9] with a slope $\tau_{RS} = 2/(\gamma_1 + \gamma_2)$, where γ_1 (γ_2) is the width of the CP-even (CP-odd) decay eigenstate D_1 (D_2) defined in Sec. 2. The decay-time distributions for the D^0 decays into the CP-even final states K^-K^+ and $\pi^-\pi^+$ are exponential with slope $\tau_{KK} = \tau_{\pi\pi} = 1/\gamma_1$.

Then, in the absence of CP violation, $y = \Delta\Gamma/2\Gamma = y_{CP}$ with:

$$y_{CP} = \frac{\tau_{RS}}{\tau_{KK}} - 1 \qquad \text{or} \qquad y_{CP} = \frac{\tau_{RS}}{\tau_{\pi\pi}} - 1. \tag{7}$$

In the available measurements $y = y_{CP}$ is assumed.[f]

3.2 Measurement of the time evolution of hadronic WS D^0 decays

The D^0 can arrive at a WS hadronic final state in two ways, either by undergoing directly the DCS decay or by first oscillating into a $\overline{D^0}$ that then undergoes a CF decay. This gives rise to three different components in the WS decay: from the DCS decay, from mixing and from the interference of the decays with (CF) and without (DCS) mixing.

Assuming CP conservation and expanding the decay rate up to $\mathcal{O}(x^2)$, $\mathcal{O}(y^2)$ results in the following approximation [7, 9] for the time evolution[g] of the hadronic[h] WS decay rate:

$$\Gamma_{WS}(t) \;\propto\; \exp(-t)\;[\; R_D \;+\; \sqrt{R_D}\; y'\; t \;+\; 1/4\;(\; x'^2 \;+ y'^2 \;)\; t^2\;], \tag{8}$$

while for the RS decays: $\Gamma_{RS}(t) \;\propto \exp(-t)$. Here, t is given in units of the lifetime of the D^0. In this approximation, the time-independent coefficient R_D corresponds to the DCS component. Even if the mixing contribution, quadratic in t, is very small, the interference term, linear in t, may result in a discernible deviation from the exponential time evolution characterizing a pure decay.

[f] If CP violation is present, then $y \neq y_{CP}$ and $y_{CP} = y\cos\phi - 0.5xA_M\sin\phi$, where A_M, ϕ are CP violating parameters related to CP violation in mixing (A_M) and in the interference of decays with (CF) and without (DCS) mixing (ϕ) [9].

[g] This formula is valid for $t \lesssim \Delta\Gamma$.

[h] Semileptonic WS D^0 decays can only arise via mixing, so that $\Gamma^{sl}_{WS}(t) \;\propto \exp(-t)(\; x^2 \;+ y^2 \;)\; t^2$.

The parameters x' and y' are related to the mixing parameters x, y by a rotation:

$$x' \;=\; x\;\cos\delta_{K\pi}\;+y\;\sin\delta_{K\pi}, \qquad y' \;=\; y\;\cos\delta_{K\pi}\;-x\;\sin\delta_{K\pi}. \tag{9}$$

The phase, $\delta_{K\pi}$, is a strong phase between the DCS contribution and the CF one and does not violate CP symmetry.

In a measurement based on the time-evolution of the WS rate alone, it is not possible to determine the phase, $\delta_{K\pi}$. Furthermore, since only the square of x' enters into $\Gamma_{WS}(t)$, the sign of x' cannot be determined, either.

If there is CP violation in the D^0 system, then the parameters R_D, x', y' in Eq. 8 have to be substituted by: $R_D^{\pm} = \sqrt{(1 \pm A_D)/(1 \mp A_D)}R_D$, $x'^{\pm} = \sqrt[4]{K^{\pm}}(x'\cos\phi \pm y'\sin\phi)$, $y'^{\pm} = \sqrt[4]{K^{\pm}}(y'\cos\phi \mp x'\sin\phi)$, where $K^{\pm} = (1 \pm A_M)/(1 \mp A_M)$. The plus (minus) sign pertains to the decay of a D^0 ($\overline{D^0}$). The three additional parameters are related to CP violation in the DCS decay (A_D), in the mixing term (A_M) and in their interference (phase ϕ) [9].

CLEO [7] in its analysis uses a somewhat different approximation which is valid for $A_D, A_M \ll 1$: $R_D^{\pm} = (1 \pm A_D)R_D$, $x'^{\pm} = \sqrt{1 \pm A_M}(x'\cos\phi \pm y'\sin\phi)$, $y'^{\pm} = \sqrt{1 \pm A_M}(y'\cos\phi \mp x'\sin\phi)$.

The total time-integrated hadronic WS rate, assuming CP conservation, is:[i]

$$R_{WS} \;=\; \int \Gamma_{WS}(t) \;/\; \int \Gamma_{RS}(t) \;=\; R_D \;+\; \sqrt{R_D}\;y' \;+\; 1/2\;(x'^2 + y'^2). \tag{10}$$

If there is no mixing in the D^0 system, then R_{WS} reflects only the rate of the DCS decay: $R_{WS} = R_D$. The SM predicts in the limit of SU(3) flavor symmetry: $R_D \sim \tan^4\theta_C \approx 0.0025$. SU(3) symmetry breaking effects may increase this value [9].

3.3 Measurement of the strong phase $\delta_{K\pi}$

No experimental determination of the strong phase, $\delta_{K\pi}$, is yet available.

Reference [10] outlines a method to extract $\delta_{K\pi}$ from a measurement of the rates of the DCS and CF decays of the type $D \to K\pi$. This method requires the determination of rate asymmetries in D meson decays to $K_L\pi$ and $K_S\pi$. In Ref. [11] Belle finds that the relevant measurements of K_L and

[i] In this approximation, the mixing rate (see Eq. 6) appears as $R_{mix} = 1/2(x'^2 + y'^2) = 1/2(x^2 + y^2)$.

K_S mesons are possible with a statistical precision sufficient to constrain $\delta_{K\pi}$ [12].

4 The experiments

The experiments BABAR and Belle at the asymmetric B-factories PEP-II and KEK-B and CLEO at the storage ring CESR operate near the $\Upsilon(4S)$ resonance at a center-of-mass energy of 10.6 GeV. PEP-II and KEK-B were designed with the primary goal of serving as asymmetric B-factories for the study of CP violation in the B^0 system. In the production cross section, $\sigma(e^+e^- \to q\bar{q}) \approx 4.45$ nb at $\sqrt{s} \approx 10.6$ GeV, $b\bar{b}$ final states account for [13] ~ 1.05 nb and $c\bar{c}$ final states for ~ 1.30 nb. In terms of production cross sections, the B-factories therefore serve equally well as charm-factories.

Between October 1999 and October 2002, BABAR recorded 94 fb^{-1} of data, while Belle recorded 98 fb^{-1}. The data set analyzed by CLEO, recorded between February 1996 and February 1999, corresponds to an integrated luminosity of 9.0 fb^{-1}. The largest available charm data sets obtained in fixed-target experiments were collected at Fermilab by the heavy-flavor photoproduction experiment FOCUS and the heavy-flavor hadroproduction experiment E791. These data sets contain $\sim 120,000$ (FOCUS) [14] and $\sim 35,000$ (E791) [15] identified $D^0 \to K^-\pi^+$ candidate events, compared to, for example, $\sim 260,000$ events [16] in the BABAR data set.

Detailed descriptions of the BABAR and Belle detectors can be found elsewhere [17, 18]. CLEO carried out its measurement with the CLEO II.V detector [19]. Of primary importance for the reconstruction and identification of D^0 decays are the vertex and particle-identification detectors. All three experiments are equipped with double-sided silicon vertex detectors. At BABAR, the Silicon Vertex Tracker (SVT) (five layers, innermost radius $r_{\rm min} = 3.2$ cm) is also capable of stand-alone track reconstruction down to particle momenta of ~ 60 MeV. Mounted just outside of the BABAR drift chamber (DCH) volume is the ring-imaging detector of internally reflected Cherenkov light (DIRC). At Belle, the Silicon Vertex Detector (SVD) (three layers, $r_{\rm min} = 3.0$ cm) and the central drift chamber are surrounded by an array of aerogel Cherenkov and time-of-flight scintillation counters (TOF). The CLEO II.V Silicon Vertex Detector (SVX) had three layers, with $r_{\rm min} = 2.35$ cm.

Differentiating kaons from pions is crucial for distinguishing with high purity between the different two-prong D^0 decays listed in Sec. 3. CLEO relies primarily on kinematic selection cuts based on the measured momenta

and the assigned mass to distinguish between the different D^0 decay modes [7, 20]. BABAR and Belle enhance their particle-identification capabilities considerably with the help of likelihoods determined from a combination of the energy-loss (dE/dx) in the tracking devices and Cherenkov detector information. Based on the ratio of the likelihoods for the two particle hypotheses, BABAR reaches an average $K^{\pm}$ identification efficiency (mis-identification probability) of $> 75\%$ ($< 8\%$) for momenta up to 4 GeV [21]. Belle includes also the TOF information in the likelihood calculation and reports an efficiency of $\sim 85\%$ and a mis-identification probability of $\sim 10\%$ for momenta up to 3.5 GeV [22].

5 Measurement of y

Following Eq. 7, the mixing parameter y is determined by measuring the slope of the decay-time distributions in independent candidate samples of $D^0 \to K^-\pi^+$ and the singly-Cabibbo suppressed channels $D^0 \to K^-K^+$ and $D^0 \to \pi^-\pi^+$.

The selection of a D^0 candidate, the determination of its proper decay-time and the general structure of the fit to obtain the D^0 lifetime from the proper decay-time distribution are discussed in some detail in the following. They are of importance also for the measurements with WS events described in Sec. 6.

5.1 Method of measurement

D^0 candidates are selected by searching for pairs of tracks with opposite charge and combined invariant mass near the expected D^0 mass. The common vertex of the track pair determines the D^0 candidate decay vertex, $\vec{v}_{dec}$, with typical resolutions as listed in Tab. 1. The interception point of the D^0 momentum vector, $\vec{p}_D$, with the envelope of the interaction point (IP) provides the production vertex, $\vec{v}_{prod}$, of the D^0 candidate [16, 20, 22].

The proper decay-time of a D^0 candidate is derived from its mass ($m_D(PDG) = 1.864$ GeV) [1] and its flight length. In order to take resolution effects properly into account, that can, e.g., result in reconstructing a negative value of t, the flight length is calculated from the projection of $\vec{v}_{dec} - \vec{v}_{prod}$ onto $\vec{p}_D$:

$$c\,t = m_D\,[\,(\vec{v}_{dec} - \vec{v}_{prod})\;\cdot\;\vec{p}_D/|\vec{p}_D|^2\,]. \tag{11}$$

The size of the IP envelope enters into the error on the proper decay-time, σ_t, through the uncertainty on the production vertex. The IP envelope is

Table 1: Comparison of parameters that enter into the calculation of the proper decay-time, t, at BABAR, Belle and CLEO [20, 21, 22].

	BABAR	Belle	CLEO
IP envelope			
vertical [μm]	6	2–4	10
horizontal [μm]	120	80–120	300
along beam-axis [mm]	8	3–4	10
resolution	80 μm	110 μm rms	40 μm
D^0 decay vtx	along $\vec{p}_D$	along $\vec{p}_D$	in each dim.
resolution of proper decay-time σ_t [fs]	180		$0.4 \times \tau_D$

smallest in the plane transverse to the beam, as shown in Tab. 1. The flight length of a D^0 candidate is typically ~ 200 μm in BABAR and Belle. The higher D^0 decay vertex resolution achieved by CLEO reflects the absence of boost-related uncertainties since at CESR, the $\Upsilon(4S)$ is produced at rest, different from PEP-II and KEK-B, where $\beta\gamma = 0.56$ and $\beta\gamma = 0.425$, respectively, along the beam direction.

5.2 Event selection

The three experiments use a similar set of quantities to reduce backgrounds [16, 20, 22]. The main differences lie in whether a $D^\star$ tag is required and which requirements are imposed for particle identification.

BABAR and CLEO select events likely to contain a D^0 with the help of the decay $D^{\star\pm} \to D^0\pi^\pm$, where the $\pi^\pm$ has very low momentum ("slow pion", π_s). Each π_s candidate track is refitted with the constraint to coincide with the D^0 candidate production vertex, determined as described in Sec. 5.1. This reduces substantially the mismeasurement of the π_s momentum caused by multiple scattering. Then the difference in the invariant mass of the $D^\star$ and the D^0 candidate, δm, is required not to deviate from the nominal one by more than a certain margin. In BABAR, this margin is 2 or 3 MeV, depending on whether the π_s reached the DCH; in CLEO the margin is 1 MeV. Belle does not use a $D^\star$ tag and requires solely that the D^0 candidate flight path be consistent with originating at the IP.

All three experiments reject events with secondary charm production from B meson decays by requiring a minimum center-of-mass momentum of the $D^\star$ or D^0 candidates (2.5 GeV for BABAR and Belle, 2.3 GeV for CLEO).

Table 2: Data samples used by BABAR, Belle and CLEO in their measurements of y [16, 20, 22].

	BABAR	Belle	CLEO
$\mathcal{L}$ [fb^{-1}]	57.8	23.4	9.0
$K^-\pi^+$ candidate events	158,000	214,000	20,300
Purity [%]	99	87	91
K^-K^+ candidate events	16,500	18,300	2,500
Purity [%]	97	67	49
$\pi^-\pi^+$ candidate events	8,400	–	930
Purity [%]	92	–	71

All three experiments reduce background from random combinations of two tracks forming a D^0 candidate with the help of the angle $\theta^\star$, measured in the D^0 candidate center-of-mass system, between the direction of the D^0 ($\overline{D^0}$) candidate boost and its positive (negative) daughter. BABAR requires $\cos\theta^\star > -0.75$ for pion daughters; Belle requires $\cos\theta^\star > -0.85$ for pion and, in the K^-K^+ channel, $|\cos\theta^\star| < 0.9$ for kaon daughters; CLEO requires $|\cos\theta^\star| < 0.8$ in all cases. BABAR and Belle apply in addition their particle-identification algorithms to the daughters of the D^0 candidate. CLEO requires in addition that the invariant mass obtained with the other possible particle-type assignments for the two daughters should be more than four standard deviations away from the nominal D^0 mass.

The analyses by BABAR and Belle reported here refer only to a sub-sample of their full data sets. The sub-sample sizes and the number of events after the full event selection are listed in Tab. 2. The purities quoted there refer to a window around the mean D^0 mass. The window size is ± 20 MeV in BABAR, $\pm 3\sigma$ in Belle ($\sigma(K^-\pi^+) = 6.5$ MeV, $\sigma(K^-K^+) = 5.4$ MeV) and ± 40 MeV in CLEO. Although BABAR's data sample corresponds to twice the integrated luminosity of Belle's, Belle's D^0 candidate event samples are larger than BABAR's and have lower purities because Belle does not require a $D^\star$ tag in its event selection. CLEO arrives at lower efficiencies and, for the CP-even channels, lower purities because CLEO, lacking dedicated particle-identification detectors, relies primarily on kinematic selection cuts to distinguish between the different D^0 decay modes.

5.3 Lifetime fit

The three experiments determine y from unbinned maximum-likelihood fits to the distribution of the reconstructed proper decay-time, t, (see Eq. 11) of the D^0 candidates [16, 20, 22]. No background subtraction is performed before carrying out the fits; rather, it is left to the fit to describe both signal and background.

The three experiments proceed in a comparable way to define the full fit function: For each of the D^0 decay channels, they define a likelihood function as the sum of a signal and a background part. Both parts consist of a decay-time distribution convolved with a resolution function. The signal decay-time distribution is exponential with a slope that corresponds to an inverse lifetime. The background decay-time distribution consists of two components, an exponential and a delta function, that model background events with non-zero and with zero lifetime, respectively. The former can, for example, arise from only partially reconstructed three-prong D^0 decays; the latter corresponds to combinations of particles into a D^0 candidate that in fact originate at the IP.

The resolution functions need to accommodate correctly reconstructed events and also events with misreconstructed parameters. This need is typically met by adding one or more Gaussians to accommodate events that are misreconstructed to varying degree. The width of the Gaussian(s) modeling the resolution of well reconstructed events is typically given by the per-event error on the reconstructed proper time t, σ_t, multiplied with a proportionality factor. The use of σ_t allows to take into account the uncertainty from the highly elliptical shape of the IP envelope (see Sec. 5.1) in the fit.

All three experiments determine the parameters of the background part of the likelihood fit function independently of those in the signal part. Also, all three experiments enhance the ability of their fits to differentiate signal from background events by multiplying the likelihood function with a per-event probability to be a signal event. The further away its reconstructed mass, m_D, is from the D^0 mass peak, the less likely is the D^0 candidate to belong to the signal. The probability is derived from an independent fit to the m_D distribution in each D^0 decay channel.

The window in m_D used in the fit must be chosen such that, in addition to the D^0 signal peak, sufficiently wide sidebands are included so that the fit can extract information on shape and size of the background. BABAR uses mass windows of 140 MeV width, defined such that reflection peaks, e.g., from mis-identified $K^-\pi^+$ events in the K^-K^+ and $\pi^-\pi^+$ candidate samples, are excluded. Belle uses a mass window of ± 40 MeV around the

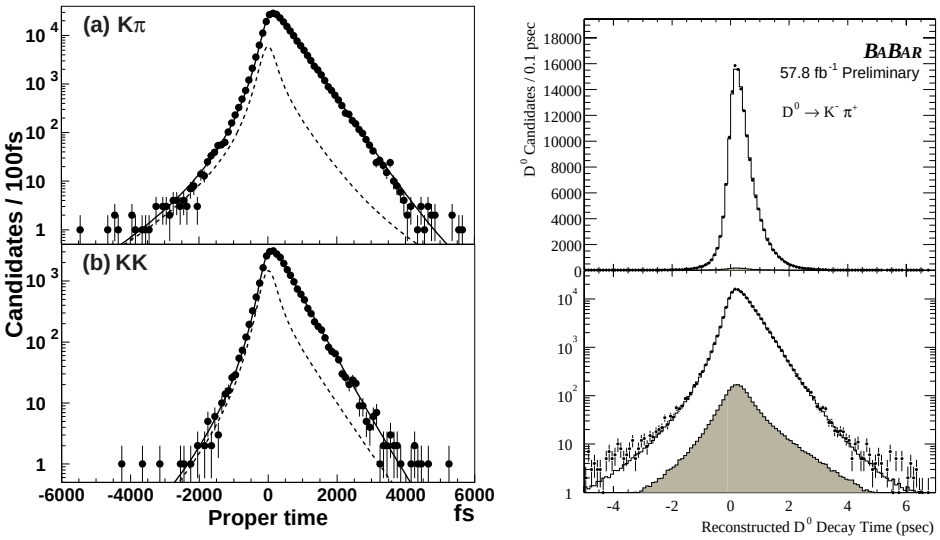

Figure 2: Proper decay-time distribution and fit result. The dots represent the data points with statistical error bars. Left: Belle [22]: For $D^0 \to K^-\pi^+$ (a) and $D^0 \to K^-K^+$ (b), in the D^0 mass signal region $\pm 3\sigma$ around the mean D^0 mass. The solid line is the result of the fit, the dashed line indicates the background contribution. Right: BABAR [16]: For $D^0 \to K^-\pi^+$, on a linear (upper) and logarithmic (lower) scale for all events including the D^0 mass sidebands. The solid line is the result of the fit, the gray area indicates the contribution attributed to background by the fit.

mean and CLEO uses the window [1.825, 1.905 GeV]. The fit results for BABAR and Belle are shown in Fig. 2. The tail at negative values in the t distribution reflects the effect of the resolution. Comparing data and fit result in the unphysical region $t < 0$ provides information about how well the resolution in the data is modeled by the fit function. The distribution for $t > 0$ reflects the resolution function convolved with the decay-time function.

5.4 Discussion of systematic uncertainties and results

Belle [22] determines y from the lifetimes measured in D^0 decays into K^-K^+ and $K^-\pi^+$ (y_{KK}). BABAR [16] and CLEO [20] use in addition the $\pi^-\pi^+$ channel ($y_{\pi\pi}$).

Belle and CLEO correct the lifetimes measured in the individual decay channels for small biases found with the help of Monte Carlo (MC) studies. Belle reports that the proper decay-time tends to be reconstructed slightly too small by a decay-channel dependent value. The resulting correction to

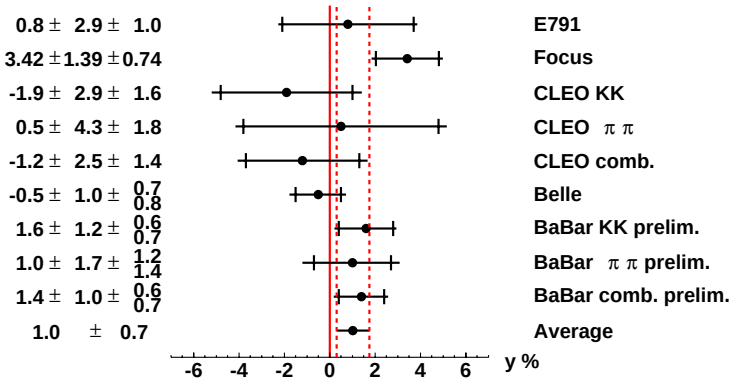

Figure 3: Comparison of results for y from different experiments [14, 15, 16, 20, 22]. The total size of the error bars corresponds to the quadratic sum of statistical and systematic error, the inner part indicates the size of the statistical error only. The average is calculated as mean of the individual measurements, each weighted by the quadratic sum of its statistical and systematic error.

y is $(-0.3 \pm 0.3)\%$. The error on this correction, due to the limited MC statistics, enters in the final systematic error on the measurement. CLEO finds bias values in the individual lifetimes that are compatible, within the statistical uncertainty on the MC bias estimate, with zero, chooses to apply corrections nonetheless and includes their statistical uncertainty in the final systematic error ($\pm 1.0\%$ for y_{KK}, $\pm 1.4\%$ for $y_{\pi\pi}$). BABAR also finds bias values compatible with zero and does not apply any corrections to the lifetimes but includes in the systematic error on y the statistical uncertainty on the MC bias estimate ($^{+0.4}_{-0.6}\%$ for y_{KK}, $^{+0.4}_{-0.9}\%$ for $y_{\pi\pi}$).

Since y is measured from the ratio of lifetimes, many systematic effects that affect the individual lifetimes do not affect y. Both Belle and CLEO find that the dominant remaining systematic error source is their understanding of the background contribution to the signals. In BABAR, the dominating source of systematic error is the above quoted uncertainty on the MC bias estimate.

All three experiments arrive at their final systematic error estimate by summing in quadrature the contributions of the individual sources. BABAR and CLEO each determine y as weighted mean of their measured y_{KK} and $y_{\pi\pi}$ values.

The results are listed in Fig. 3. Also shown are results from the fixed-target experiments[j] FOCUS [14] and E791 [15]. Within their errors, the

[j]The fixed-target experiment results are obtained by means of a fit to the reduced

results are compatible with each other and with the SM expectation of a value of $|y|$ close to zero.

6 Measurements with the WS decays $D^0 \to K^+\pi^-$, $\overline{D^0} \to K^-\pi^+$

As discussed in Sec. 3.2, the time evolution of the WS decay rate provides a means of measuring simultaneously x'^2 and y'. CLEO has published a result [7] obtained with 9.0 fb^{-1} of data. BABAR has presented a preliminary analysis [21] based on a data sample of 57.1 fb^{-1}. At Belle, work to extract the time evolution of WS events is on-going [12]; results concerning the background in the WS sample have already been presented [23], but none yet on x'^2, y'. All three experiments have results for the time-integrated WS decay rate R_{WS} [7, 21, 23].

6.1 Extraction of x', y' from the time evolution of the WS decay rate

Wrong-sign candidate events of the type $D^0 \to K^+\pi^-$ and $\overline{D^0} \to K^-\pi^+$ are selected by requiring the π_s from the $D^\star$ decay and the daughter K of the D^0 to have identical charge (WS tag). In addition, CLEO, BABAR and Belle apply event selection criteria similar to those described in Sec. 5.2, and the proper decay-time is reconstructed as discussed in Sec. 5.1 [7, 21, 23].

The measurement aims at detecting a deviation from a purely exponential decay law in WS events (see Sec. 3.2) by means of a likelihood fit to the distribution of the reconstructed proper decay-time, t. The likelihood functions used by the experiments have the same principal structure as the ones used in the measurement of y (see Sec. 5.3). They differentiate between a signal and a background component and model each as the convolution of a decay-time distribution and a resolution function. For WS events, the decay-time distribution follows Eq. 8, i.e. includes the three parts discussed earlier: DCS decay, mixing and interference between the decays with (CF) and without (DCS) mixing.

The WS sample has only $\sim 1/300$ times the number of events of a RS sample selected with the same criteria as the WS sample except for the WS

proper time. This quantity includes a cut on a minimum distance between primary and secondary vertex as a principal tool to reduce non-charm background and is measured with a resolution of less than 1/10 of the D^0 lifetime. The FOCUS (E791) result on y is derived from $\sim 120,000$ ($\sim 35,400$) events in the $K^-\pi^+$ channel and $\sim 10,300$ ($\sim 3,200$) events in the K^-K^+ channel.

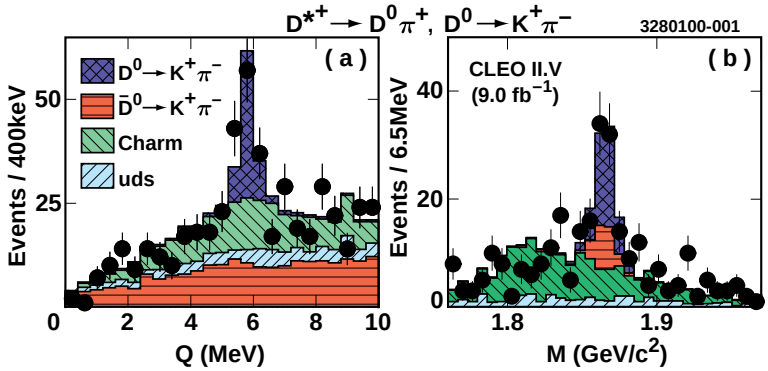

Figure 4: Signal (dots, with statistical error bars) observed by CLEO [7] for the WS decay $D^0 \to K^+\pi^-$ (charge conjugate mode included). The projections of the fit for the signal (cross-hatched) and the background (background of type A - "uds", type B - "charm", type C - "$\overline{D^0} \to K^+\pi^-$") is shown. M (left) and Q (right) are each within 2σ of their mean in the RS mode.

tag. This RS sample is used wherever possible to constrain aspects in the fit that are common to the two samples. CLEO and BABAR determine, e.g., the resolution functions of WS and RS signals and of the common background types with the RS sample.

In the WS sample, a significant additional complication arises from the much lower achievable purity[k], e.g. $\sim 50\%$ in the CLEO analysis. The fit needs to accord each background type its specific lifetime evolution, distinct from the ones of the other background types and from those of the signal events. The reconstructed m_D and δm distributions provide a means of differentiating between the different background types and between background and signal.

6.1.1 Fitting procedure

CLEO performs a two-step fitting procedure. First, the levels of the different background types in the selected candidate sample are estimated by performing a fit to the two-dimensional region $1.76 < m_D < 1.97$ GeV and

[k] A rough estimate can be obtained by assuming that in a given random sample of events, the probability for a non-signal event to be mis-identified as a signal event is the same for WS and RS signal. Then, a purity of 99% in the RS candidate sample translates into a purity of 25% in the WS candidate sample because WS events are 300 times less frequent than RS events. This simplified example does not include background from random π_s that together with a CF D^0 decay mimic a WS event.

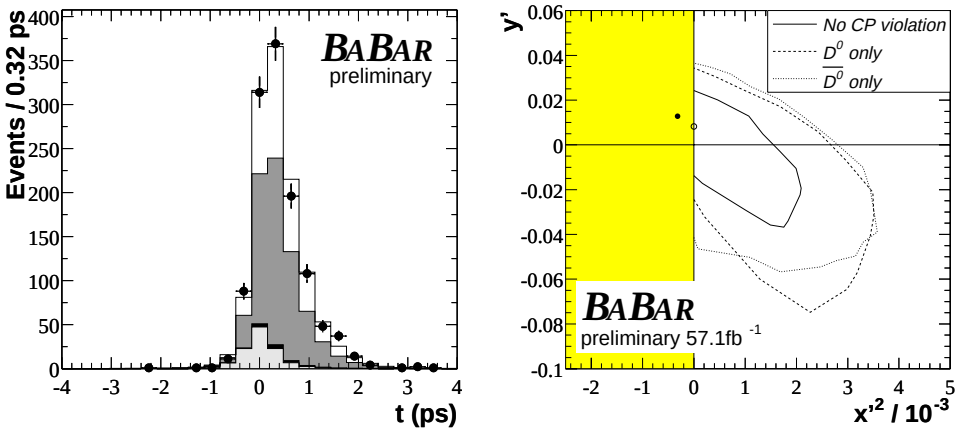

Figure 5: (a) Distribution of the proper decay-time, t, in the WS data sample (dots) compared to the fit result for the different background types (A: light grey, B: black, C: darker grey) and for the signal (open). (b) 95% C.L. contours, including the systematic uncertainty, for D^0 and $\overline{D^0}$ separately (combined) when (when not) allowing for CP violation. The solid (open) point represents the most likely fit point in the case of no CP violation without (with) the constraint $x'^2 > 0$ [21].

$0 < Q < 10$ MeV, where $Q = \delta m - m_\pi$ and m_π is the pion mass. CLEO differentiates three types of backgrounds: A) from the CF decay that together with a random π_s^+ mimics a WS event ("$\overline{D^0} \to K^+\pi^-$"), B) with non-zero lifetime ("charm") and C) with zero lifetime ("uds"). The background shapes in the $m_D - \delta m$ plane are estimated with the help of a Monte Carlo sample that corresponds to $\mathcal{L} = 90$ fb^{-1}. The signal shape is constrained with the help of the RS sample. The fit yields ~ 45 WS signal events in the total of 82 selected candidate events, measured within a 2σ window around the central values of the m_D and Q distributions. ($\sigma(m_D) = 6.4 \pm 0.1$ MeV and $\sigma(Q) = 190 \pm 2$ keV). Figure 4 shows the observed signal as function of Q and $M = m_D$ together with the projected background estimates from the fit. In the second step, CLEO performs a binned maximum-likelihood fit (bin size 1/20 of the D^0 lifetime) to the distribution of the proper decay-time, t. In this fit, the background levels from the first fit in the $m_D - \delta m$ plane are used.

BABAR performs an unbinned maximum-likelihood fit in several steps. First, the number of signal and background events is determined in a fit to the $m_D - \delta m$ plane. In the WS sample, BABAR models separately the background from A) the CF decay that together with a random π_s mimics

a WS event, B) RS events where the K and π hypotheses are swapped, C) purely combinatorial background. In the RS sample, BABAR considers in addition background from D) partially reconstructed D^0 mesons, typically from 3-prong D^0 decays. The δm distributions for background types A) and C) are obtained directly from the data by means of mixing a π_s from a $D^\star$ decay of one event with the D^0 candidate of another event. The fit yields $\sim$ 440 signal WS events in the region $1.804 < m_D < 1.924$ GeV, $\delta m < m_\pi + 25$ MeV. Figure 5(a) shows the reconstructed proper decay-time distribution for the WS signal and the three background types A)–C). In a second step, a fit to the RS and WS proper decay-time distributions is performed simultaneously to determine the resolution functions.

Belle has reported results on the first part of the fitting procedure, the two-dimensional fit in the $m_D - \delta m$ plane. Belle considers background types similar to BABAR's. Specifically to suppress background type B), Belle requires that the invariant mass of the D^0 candidate calculated with swapped particle hypotheses for the daughters differs from the nominal mass by more than 28 MeV ($\sim 4\sigma$). The remaining background types are modeled in the $m_D - \delta m$ plane fit function. The fit arrives at $\sim$ 450 WS signal events in the region $1.81 < m_D < 1.91$ GeV, $0 < Q < 20$ MeV. Belle has not yet released any results from the fit to the distribution of the proper decay-time, t.

For the WS decay-time function, CLEO and BABAR both follow Eq. 8 and consider the case with and without CP violation. Input to all fits is m_D, δm, t, σ_t.

6.1.2 Discussion of results

The results of both CLEO [7] and BABAR [21] are consistent with the absence of mixing and of CP violation.

CLEO constructs contours in the $x' - y'$ plane that contain the true value of x', y' with 95% confidence. Following a Bayesian [1] approach, the 95% confidence region includes all points in the plane for which the negative log likelihood, $-\ln L$, differs from the best fit value by more than 3.0. All fit variables other than x', y' are allowed to vary to give the best fit value at each point on the contour. The 95% confidence region, when not and when allowing for CP violation, is shown in Fig. 6(a). There, the assumption $\delta_{K\pi} = 0^\circ$ is made for the strong phase (see Eq. 9), so that $x' = x$ and $y' = y$. The contours do not include any estimate of systematic errors. CLEO also quotes one-dimensional limits at the 95% C.L. for the mixing parameters, $(1/2)x'^2 < 0.041\%$ and $-5.8\% < y' < 1.0\%$, without assumptions on CP violation. CLEO identifies as its dominant source of systematic error the

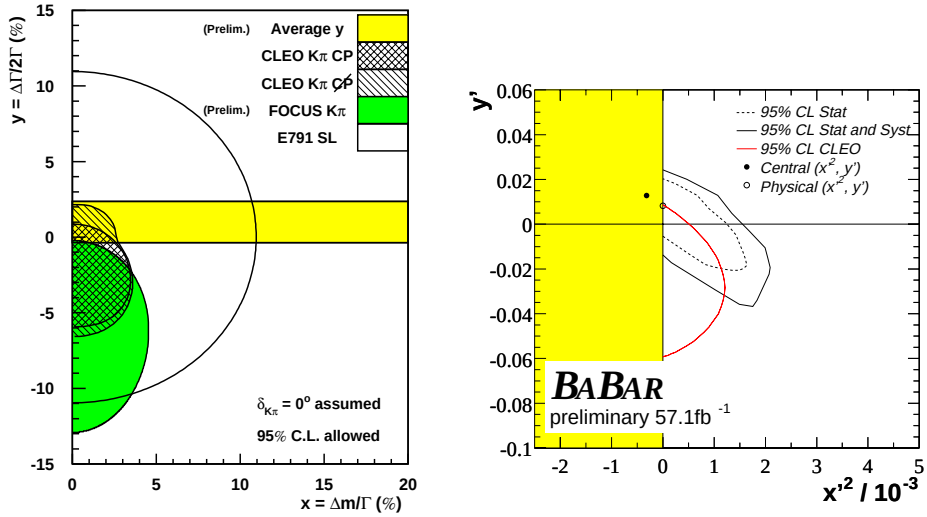

Figure 6: (a) Comparison of the 95% C.L. contours in the $x - y$ plane from E791 [25], FOCUS [26] and CLEO [7]. For the bigger kidney-shaped (smaller) region from CLEO, CP violation was (was not) allowed in the fit. Also shown is the band corresponding to the current average for y obtained in lifetime-difference analyses (see Fig. 3). The assumption $\delta_{K\pi} = 0°$ for the strong phase is made. (b) Comparison of the 95% C.L. contours in the $x'^2 - y'$ plane from CLEO and BABAR when assuming CP conservation in the fit. The CLEO contour does not include systematic uncertainties.

potential misunderstanding of the background shapes and acceptances and assigns a total systematic error of $\pm 0.2\%$ ($\pm 0.3\%$) for x' (y').

Figure 6(a) also shows a preliminary contour from FOCUS [26], derived from an analysis of WS hadronic decays of the type $D^0 \to K^+\pi^-$, a 95% C.L. contour from E791 [25], derived from the 90% C.L. limit $R_{mix} < 0.50\%$[1] in WS semileptonic decays of the type $D^0 \to K^+ l^- \nu_l$, and the band corresponding to the average on y from the lifetime difference analyses (see Fig. 3). Not shown is the contour from E791 [24] derived from the weaker 90% C.L. limit $R_{mix} < 0.85\%$ in WS hadronic decays of the type $D^0 \to K^+\pi^-$ and $D^0 \to K^+\pi^-\pi^+\pi^-$.

BABAR uses a method different from CLEO's to arrive at a 95% C.L. contour. BABAR argues that due to allowing x'^2 in its fit to take unphysical negative values, it is not clear how to apply a Bayesian ansatz to derive

[1] $R_{mix} \approx 1/2(x'^2 + y'^2) = 1/2(x^2 + y^2)$.

Table 3: Comparison of the 95% C.L. limits for the fit output parameters of BABAR and CLEO when CP conservation is assumed in the fit. BABAR's limits include systematic uncertainties and were obtained in a fit that allowed $x'^2 < 0$.

	R_D	y'	x'	x'^2
CLEO [%]	(0.24, 0.69)	(-5.2, 0.2)	(-2.8, 2.8)	< 0.076
BABAR [%]	(0.22, 0.46)	(-3.7, 2.4)	-	< 0.21

an error estimate from the two-dimensional likelihood distribution. In addition, BABAR finds that the likelihood distribution depends strongly on the most likely fitted values of x'^2 and y'. To define 95% C.L. contours, BABAR applies a frequentist approach based on toy Monte Carlo (MC) experiments. Any point $\vec{\alpha_c} = (x'^2_c, y'_c)$ on the 95% C.L. contour has to meet the requirement: If a toy MC experiment is generated at that point, there is a 95% probability that the ratio $\Delta \ln L(\vec{\alpha_c}) = \ln L(\vec{\alpha_c}) - \ln L_{max}$ is greater than $\Delta \ln L_{data}(\vec{\alpha_c})$ calculated for the data. There, L_{max} is the maximum likelihood obtained in the fit either to data or to a toy MC sample. BABAR constructs 95% C.L. contours also for the systematic effects considered in the analysis, among them uncertainties in the form of the fit functions, detector effects and effects of the selection criteria. Figure 5(b) shows the resulting 95% C.L. contours that include the statistical as well as the systematic uncertainty estimate. A strong correlation between x'^2 and y' is apparent. The most likely fit point in the case of no CP violation has a negative coordinate in x'^2.

A direct comparison of the CLEO and BABAR results is not possible for the case when CP violation is allowed in the fit. CLEO uses as fit output parameters x', y', R_D and A_D, A_M, $\sin\phi$, while BABAR uses x'^{+2}, y'^{+}, R^+ (x'^{-2}, y'^{-}, R^-) for the D^0 ($\overline{D^0}$) case (see Sec. 3.2).

The results when assuming CP conservation in the fit are in principle comparable between CLEO and BABAR, see Tab. 3. BABAR includes systematic uncertainties in its 95% C.L. contour and obtains its limits on x'^2 and y' by projecting this contour onto the corresponding axis. The CLEO limits in Tab. 3, instead, correspond to one-dimensional 95% C.L. intervals, determined by an increase in $-\ln L$ of 1.92 compared to the best fit value, and do not include systematic uncertainties.

BABAR's upper limit on x'^2 is almost three times bigger than CLEO's, in spite of being based on a six times larger data sample. A possibly overly conservative estimate of the systematic error cannot account for a difference of this size, as illustrated by Fig. 6(b). There, the CLEO 95% C.L. contour

(no systematic errors) is overlaid with the two BABAR contours that are obtained before and after adding the systematic uncertainty. Two possible reasons for so pronounced a difference between CLEO and BABAR are the different techniques for obtaining the 95% C.L. limits and the treatment of the fit output parameter x'. BABAR allows x'^2 to take unphysical negative values in its fit, while CLEO excludes this possibility by choosing x' instead of x'^2 as fit parameter. Another possible reason is the sign of the fit result on y'. Toy Monte Carlo studies indicate that the 95% C.L. contour differs in size and shape depending on the sign [12, 27]. For positive y' (the BABAR case), the contour tends to be larger than for negative y' (the CLEO case). Albeit its precise origin is not yet understood, this behavior may point to a qualitative difference between the two regimes, with destructive (constructive) interference between the decays with (CF) and without (DCS) mixing for $y < 0$ ($y > 0$).

6.2 Extraction of the time-integrated WS decay rate R_{WS}

CLEO and BABAR arrive at a measurement of R_{WS} by repeating the fits described above with the assumption of no mixing in the D^0 system, i.e. $x = y = 0$ [7, 21].

Belle uses its fit in the $m_D - \delta m$ plane, described above, to determine the time-integrated number of signal events in the candidate samples [23]. The ratio of the number of signal events in the WS and RS candidate samples yields R_{WS}. The systematic error on R_{WS} is dominated by the uncertainty on the background shapes used in the fit.

Figure 7 compares the results from CLEO [7], based on $\mathcal{L} = 9.0$ fb^{-1}, BABAR [21] (57.1 fb^{-1}) and Belle [23] (46.2 fb^{-1}) to earlier measurements by E791 [24], ALEPH [28] and FOCUS [29] in WS decays of the type $D^0 \to K^+\pi^-$.

In the absence of mixing, R_{WS} corresponds to the the doubly Cabibbo-suppressed decay rate R_D (see Sec. 3.2). The discrepancy between the SM expectation in the absence of mixing, $R_D \approx 0.25\%$, and the values of R_{WS} measured by CLEO, BABAR and Belle may be attributable to the effect of SU(3) symmetry breaking [9].

7 Summary and Outlook

The asymmetric B-factories PEP-II and KEK-B with the experiments BABAR and Belle, operational since 1999, have rendered possible studies of mixing

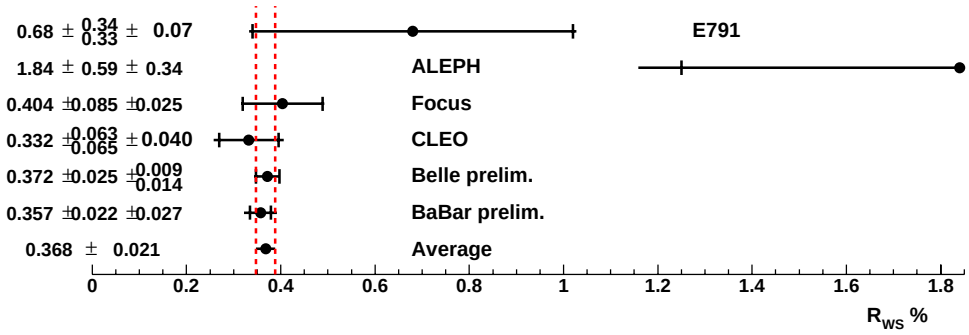

Figure 7: Comparison of results for R_{WS} from different experiments [7, 21, 23, 24, 28, 29]. The total size of the error bars corresponds to the quadratic sum of statistical and systematic error, the inner part indicates the size of the statistical error only. The average is calculated as mean of the individual measurements, each weighted by the quadratic sum of its statistical and systematic error.

in the D^0 system with unprecedented statistical precision and sample purities. First results for the mixing parameters x and y are compatible with an absence of mixing and of CP violation.

BABAR and Belle both expect to reach $\mathcal{L} = 500$ fb^{-1} by 2006. In data sets of this size, the statistical errors in the measurements reviewed in this article can be reduced by a factor of three. For y, a statistical precision of $\sim 0.2\%$ would be within reach and could be further improved by, e.g., employing additional D^0 decay channels of well-defined CP symmetry and, for BABAR, by investigating the possibility of dropping the $D^\star$ tag requirement in its event selection.

BABAR's preliminary result for x'^2, y', determined from the time evolution of WS decays of the type $D^0 \to K^+\pi^-$, is the second such result from a collider experiment after CLEO's. Already with its present data sample, BABAR should be able to improve its systematic error estimate substantially. Future results from Belle should help shedding light on the differences between the CLEO and the BABAR result. Additional information may be gained from other WS D^0 decay channels, hadronic and semileptonic ones, which have already been observed in other experiments (see e.g. Ref. [24, 30]).

Given the huge uncertainties in Standard Model (SM) predictions for D^0 mixing, it might prove difficult to establish physics beyond the SM from the size of the measured x and y parameters alone. A more robust potential signal for new physics may well be CP violation in the D^0 system [3]. Efforts

to establish CP violation in the D^0 system are already part of the WS time evolution analyses discussed in this review and are likely to intensify in the future.

Methods for investigating mixing in the D^0 system complementary to those at the B-factories would be available at CLEO-c. CLEO-c at CESR-c, currently under discussion as successor to CESR at Cornell, may operate at the $D^0\overline{D^0}$ threshold. There, the quantum-mechanical coherence of the produced D^0, $\overline{D^0}$ pair can be exploited to study mixing in the D^0 system in ways not available[m] to any already existing experiment [31, 32].

Acknowledgments

I would like to thank Ulrik Egede and Bruce Yabsley for enlightening discussions, helpful suggestions and feedback on this review. The help of the BABAR, Belle, CLEO and FOCUS collaborations by making available several figures for inclusion in this review is gratefully acknowledged, as is the help of Harry Cheung in preparing Fig. 6(a). I would also like to thank Tom Browder, Pat Burchat, Nick Ellis, Brian Meadows, Abe Seiden and David Williams for their comments on the manuscript.

References

[1] Particle Data Group, K. Hagiwara et al., *Phys.Rev.* **D66**, 010001 (2002).

[2] A.F.Falk, Y.Grossman, Z.Ligeti, A.A.Petrov, *Phys.Rev.* **D65**, 054034 (2002).

[3] A.A.Petrov, "CP violation and mixing in charmed mesons", Proc. of Continuous Advances in QCD 2002/ARKADYFEST, May 2002, hep-ph/0209049.

[4] H.N.Nelson, "Compilations of D^0 - $\bar{D^0}$ mixing predictions", Proc. 19th Int. Symposium on Lepton and Photon Interactions at High-Energies (LP 99), Stanford CA, USA, Aug. 1999, hep-ex/9908021.

[5] R.Waldi, *Prog.Part.Nucl.Phys.* **47**,1 (2001)

[m] The coherent state of the D^0, $\overline{D^0}$ pair renders possible, for example, a direct measurement of the strong phase $\delta_{K\pi}$ (see Eq. 9) between the DCS and CF decays [31, 32].

[6] J.H.Christenson, J.W.Cronin, V.L.Fitch, R.Turlay, *Phys.Rev.Lett.* **13**,138 (1964);
BABAR Collab., B.Aubert et al., *Phys.Rev.Lett.* **87**, 091801 (2001);
Belle Collab., K.Abe et al. *Phys.Rev.Lett.* **87**, 091802 (2001).

[7] CLEO Collab., R.Godang et al., *Phys.Rev.Lett* **84**, 5038 (2000).

[8] E.Golowich, Proc. of the conference on B physics and CP violation, Honolulu Hl, USA, March 1997, hep-ph/9706548.

[9] S.Bergmann, Y.Grossman, Z.Ligeti, Y.Nir, A.A.Petrov, *Phys.Lett.* **B486** 418 (2000).

[10] E.Golovich, S.Pakvasa, *Phys.Lett.* **B505**, 94 (2001).

[11] Belle Collab., K.Abe et al. , "Measurement of D^0 decays to $K^0_L\pi^0$ and $K^0_S\pi^0$ at Belle", BELLE-CONF-0129, hep-ex/0107078, July 2001.

[12] B.Yabsley, private communication.

[13] P.F.Harrison, H.R.Quinn (ed.s), The BABAR Physics Book, SLAC-R-504, 1998.

[14] FOCUS Collab., J.M.Link et al., *Phys.Lett.* **B485**, 62 (2000).

[15] E791 Collab., E.M. Aitala et al., *Phys.Rev.Lett.* **83**, 32 (1999).

[16] A.Pompili, "Charm Mixing and Lifetimes at BABAR", Proc. of the 37th Rencontres de Moriond, Les Arcs, France, March 2002, SLAC-PUB-9496, hep-ex/0205071; M.Grothe, "Results on mixing in the D^0 system from BABAR", Proc. of the 9th Int. Symposium on Heavy Flavor Physics (HF9), Pasadena CA, USA, Sept. 2001, BABAR-PROC-01/91, SLAC-PUB-9064, hep-ex/0112002.

[17] BABAR Collab., B.Aubert et al., *Nucl.Instrum.Meth.* **A479**, 1 (2002).

[18] Belle Collab., S.Mori (ed.) et al., *Nucl.Instrum.Meth.* **A479**, 117 (2002).

[19] CLEO Collab., Y.Kubota et al., *Nucl.Instrum.Meth.* **A320**, 66 (1992); T.S.Hill, *Nucl.Instrum.Meth.* **A418**, 32 (1998).

[20] CLEO Collab., S.E.Csorna et al., *Phys.Rev.* **D65**, 092001 (2002).

[21] U.Egede, "Mixing in the D^0-$\bar{D}^0$ system in BABAR", Proc. of the First Int. Workshop on Frontier Science, Frascati, Oct. 2002, SLAC-PUB-9552, BABAR-PROC-02/114, hep-ex/0210060.

[22] Belle Collab., K.Abe et al. , *Phys.Rev.Lett.* **88**, 162001 (2002).

[23] Belle Collab., K.Abe et al. , "A measurement of the rate of WS decays $D^0 \to K^+\pi^-$", BELLE-CONF-0254, hep-ex/0208051.

[24] E791 Collab., E.M.Aitala et al., *Phys.Rev.* **D57**, 13 (1998).

[25] E791 Collab., E.M.Aitala et al., *Phys.Rev.Lett.* **77**, 2384 (1996).

[26] J.M.Link, "D^0-$\bar{D}^0$ mixing in FOCUS", Proc. of the 36th Rencontres de Moriond, Les Arcs, France, March 2001, hep-ex/0106093.

[27] U.Egede, private communication.

[28] ALEPH Collab., R.Barate et al., *Phys.Lett.* **B436**, 211 (1998).

[29] FOCUS Collab., J.M.Link et al., *Phys.Rev.Lett.* **86**, 2955 (2001).

[30] CLEO Collab., G. Brandenburg et al., *Phys.Rev.Lett.* **87**, 071802 (2001).

[31] CLEO-c Collab., R.A.Briere et al., "CLEO-c and CESR-c: A New Frontier of Weak and Strong Interactions", CLNS 01/1742, Oct. 2001.

[32] M.Gronau, Y.Grossman, J.Rosner, *Phys.Lett.* **B508**, 37 (2001).